Journal of Medicinal Chemistry

Article

Synthesis and Identification of [1,3,5]Triazine-pyridine Biheteroaryl as a Novel Series of Potent Cyclin-Dependent Kinase Inhibitors

Gee-Hong Kuo, Alan DeAngelis, Stuart Emanuel, Aihua Wang, Yan Zhang, Peter J. Connolly, Xin Chen, Robert H. Gruninger, Catherine Rugg, Angel Fuentes-Pesquera, Steven A. Middleton, Linda Jolliffe, and William V. Murray

J. Med. Chem., **2005**, 48 (14), 4535-4546• DOI: 10.1021/jm040214h • Publication Date (Web): 27 May 2005

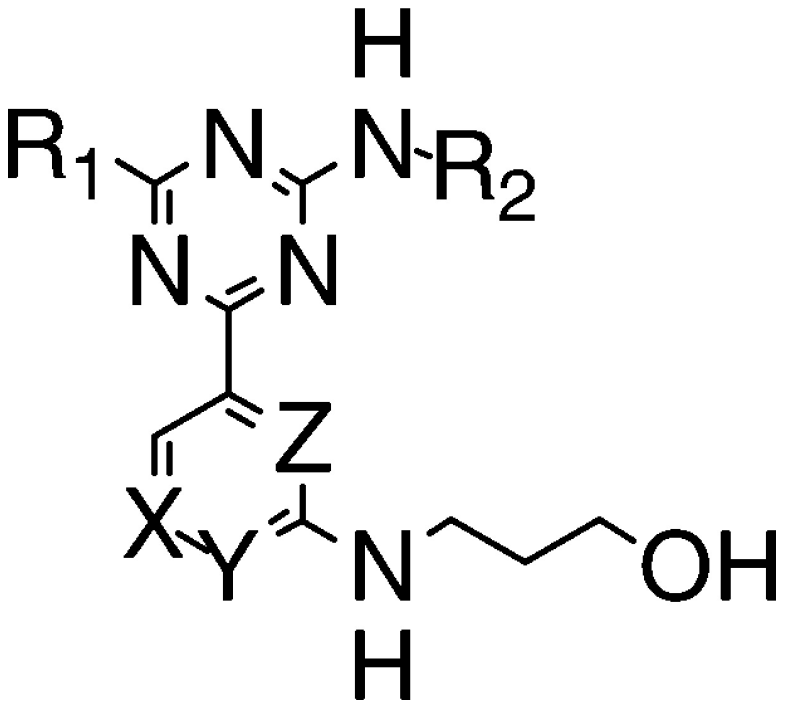

More About This Article

Additional resources and features associated with this article are available within the HTML version:

- Supporting Information
- Links to the 3 articles that cite this article, as of the time of this article download
- Access to high resolution figures
- Links to articles and content related to this article
- Copyright permission to reproduce figures and/or text from this article

Journal of Medicinal Chemistry is published by the American Chemical Society. 1155 Sixteenth Street N.W., Washington, DC 20036

Synthesis and Identification of [1,3,5]Triazine-pyridine Biheteroaryl as a Novel Series of Potent Cyclin-Dependent Kinase Inhibitors

Gee-Hong Kuo,* Alan DeAngelis, Stuart Emanuel, Aihua Wang, Yan Zhang, Peter J. Connolly, Xin Chen, Robert H. Gruninger, Catherine Rugg, Angel Fuentes-Pesquera, Steven A. Middleton, Linda Jolliffe, and William V. Murray

Drug Discovery Division, Johnson & Johnson Pharmaceutical Research and Development, L.L.C., 1000 Route 202, P.O. Box 300, Raritan, New Jersey 08869

Received December 14, 2004

On the basis of previous studies, we identified pyrazine-pyridine A as a potent vascular endothelial growth factor inhibitor and pyrimidine-pyridine B as a moderately potent cyclin dependent kinase (CDK) inhibitor. A proposed combination of CGP-60474 and compound B led to the discovery of [1,3,5]triazine-pyridine as a new series of potent CDK inhibitors. Palladium-catalyzed C−C bond formation reactions, particularly the Negishi coupling reaction, were used to assemble various triazine-heteroaryl analogues effectively. Among them, compound **20** displayed high inhibitory potency at CDK1 (IC_{50} = 0.021 μM), CDK2, and CDK5 and submicromolar potency at CDK4, CDK6, and CDK7. Compound **20** also displayed high potency at GSK-3β. It demonstrated potent antiproliferative activity on various tumor cell lines, including HeLa, HCT-116, U937, and A375. When **20** was administered intraperitoneally at 150 and 125 mg/kg to nude mice bearing human A375 xenografts, the compound produced a significant survival increase. Molecular docking studies were conducted in an attempt to enhance the understanding of the observed structure−activity relationship.

Introduction

A fundamental process in biology is the proliferation of cells mediated by the cell cycle.[1] The principal function of the cell cycle is to effect the duplication of DNA and its appropriate distribution to newly divided daughter cells. For convenience, the cell cycle has been described as having four phases: (1) G1 (gap 1), the phase in which the cell prepares for DNA synthesis, (2) S (synthesis), the phase in which DNA is replicated, (3) G2 (gap 2), the phase in which the cell prepares for mitosis, and (4) M (mitosis), the phase that leads to chromosome segregation and daughter cell formation.

Cyclin-dependent kinases (CDKs) play a key role in regulating cell cycle machinery.[2] This family of kinases requires association with a cyclin regulatory subunit for activity. Different CDK/cyclin pairs are active during each phase of the cell cycle.[3] To date, at least 9 CDKs and more than 12 different cyclin families have been identified. Critical CDKs/cyclins for core cell cycle function are CDK1/cyclin B, CDK2/cyclin A, CDK2/cyclin E, CDK4/cyclin D, and CDK6/cyclin D.[4] In addition, CDK5 activity is highest in the brain and may play a role in neurogenesis and Alzheimer's pathology[5] while CDK7, CDK8, and CDK9 have been implicated in the modulation of RNA elongation.[6]

An increasing body of evidence indicates that uncontrolled CDK activity is a common feature related to proliferative diseases such as cancer, psoriasis, and restenosis.[7] In a literature review, discovery and lead optimization efforts have provided many CDK inhibitors over the past decade.[8] Among them, UCN-01 (**34**) (Chart 1),[9,10] which is a nonspecific inhibitor of CDK1, CDK2, CDK4, protein kinase C (PKC), mitogen-activated protein kinase (MAPK), and other kinases, is currently under development (phase I/II) for the treatment of various cancers including ovarian cancer, melanoma, and leukemia.[4] Roscovitine,[11,12] a CDK1, CDK2, and CDK5 inhibitor, is in phase II clinical trials for the treatment of breast cancer and non-small-cell lung cancer. BMS-387032 **35**,[13] a CDK2, CDK1, and CDK4 inhibitor, has been investigated in a phase I clinical trial for patients with advanced refractory solid tumors. Indisulam,[14] an inhibitor of carbonic anhydrase and CDK2 phosphorylation, is in phase II clinical trials for breast, colorectal, and head/neck cancers. ZK-CDK (**36**)[15] (a CDK1, CDK2, vascular endothelial growth factor receptor (VEGFR), and platelet-derived growth factor receptor β inhibitor) is in phase I clinical trials for the treatment of solid tumors. In this article, we describe our efforts toward the identification of triazine-pyridine biheteroaryls as novel and potent CDK inhibitors that may potentially be useful for the treatment of solid tumors.

Chemistry

The 4-chloro-[1,3,5]triazine **4** was synthesized via the reaction of 2,4-dichloro-[1,3,5]triazine **3**[16] with Boc-protected aniline **2** under basic conditions (Scheme 1). The required bromide **7** was prepared in a two-step sequence: (1) a Curtius rearrangement[17] of the nicotinic acid **5** with DPPA gave **6**, and (2) alkylation of **6** with the silyl-protected bromide gave **7**. To our surprise, the palladium-catalyzed Stille coupling reaction[18] (or Suzuki coupling reaction[19]) of chloride **4** with the organostannane (or organoboron compound) prepared from bromide **7** gave only a trace amount of the coupling product. Fortunately, the palladium-catalyzed Negishi coupling

* To whom correspondence should be addressed. Tel: 908-704-4330. Fax: 908-203-8109. E-mail: gkuo@prdus.jnj.com.

10.1021/jm040214h CCC: $30.25
Published on Web 05/27/2005

Chart 1

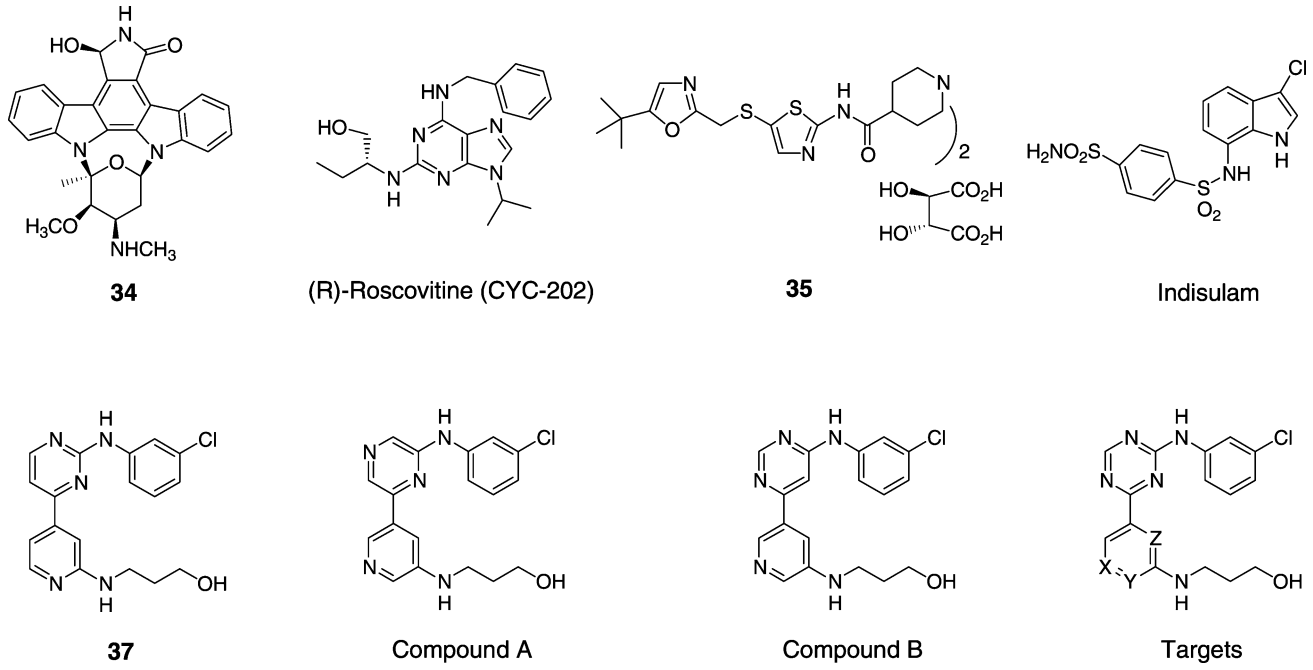

Scheme 1[a]

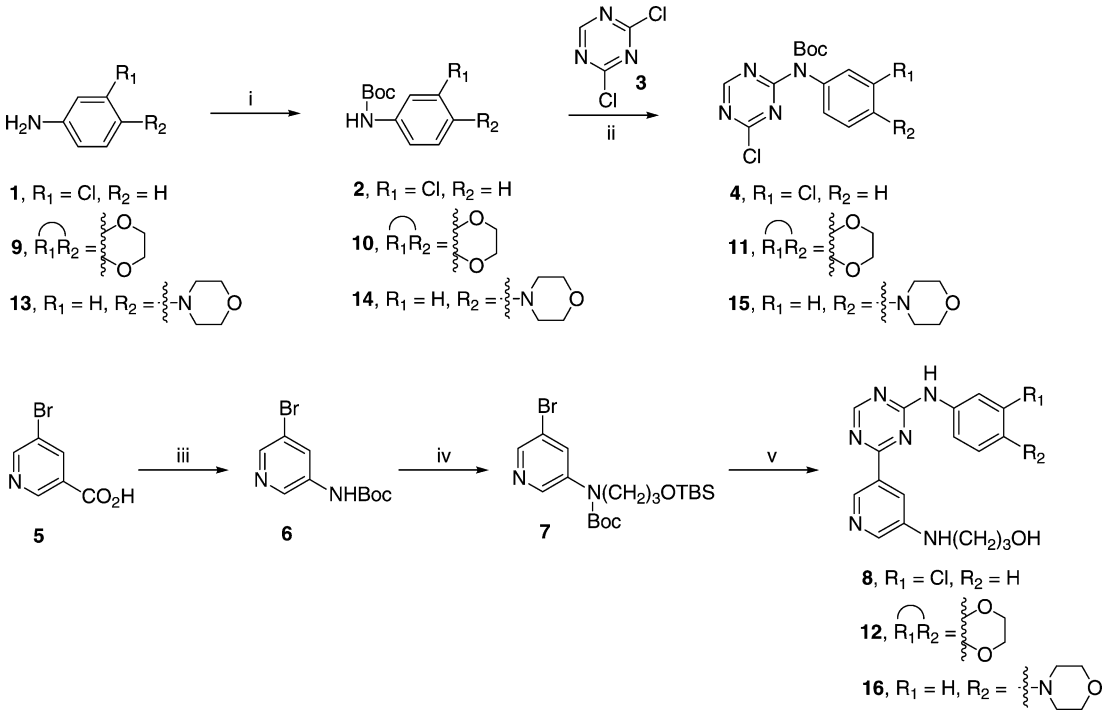

[a] (i) Boc_2O, THF; (ii) NaH, THF, **3**; (iii) DPPA, Et_3N, *t*-BuOH, 65−100 °C; (iv) $Br(CH_2)_3OTBS$, Cs_2CO_3, DMF, 70 °C; (v) (a) *n*-BuLi, $ZnCl_2$, −78−20 °C, **4** (or **11** or **15**), $Pd(PPh_3)_4$, THF, 70 °C and (b) TFA.

reaction[20] of chloride **4** with the organozinc intermediate prepared from **7** gave the desired triazine-3-pyridine coupling product **8** after deprotection with trifluoroacetic acid (TFA). The second target **12** and the third target **16** were prepared in the same manner as compound **8**.

The triazine-4-pyridine target **20** was prepared by two different methods. The first method (method A, Scheme 2) involved the reaction of **17** with *N,N*-dimethylformamide dimethyl acetal to give **18**, followed by cyclocondensation[21] of **18** with (3-chlorophenyl)-guanidine nitrate[22] to give chloride **19**. Reaction of **19** with 3-amino-1-propanol gave the desired triazine-4-pyridine **20** in modest yield. The second approach is shown in Scheme 3. A Curtius rearrangement was conducted on **21**[23] to afford **22**. Alkylation of **22** followed by the organostannane formation reaction[24] yielded **24**. A palladium-catalyzed Stille coupling reaction of **24** with chloride **4**, followed by TFA deprotection gave target **20**.

The synthesis of triazine-pyrazine **29** is shown in Scheme 4. A Curtius rearrangement of **25**[25] gave **26**. Alkylation and organostannane formation, followed by Stille coupling reaction and deprotection, afforded **29** in a manner similar to that of **20**. The synthesis of amino-triazine-4-pyridine **33** is shown in Scheme 5.

Scheme 2[a]

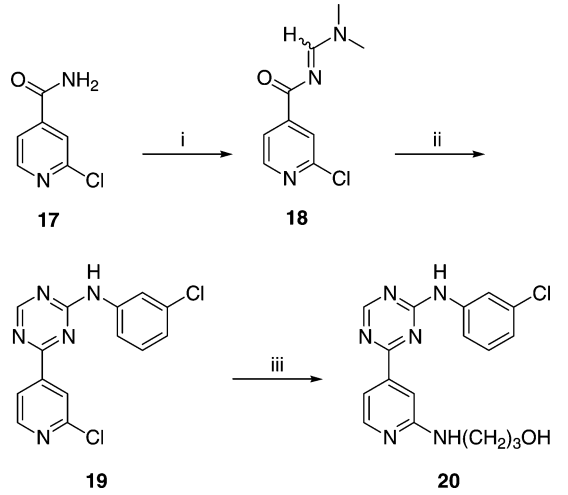

[a] (i) *N,N*-dimethylformamide dimethyl acetal, 100 °C; (ii) (3-chloro-phenyl)-guanidine nitrate, K^{t}OBu, THF, 20−70 °C; (iii) 3-amino-1-propanol, 85 °C.

Scheme 3[a]

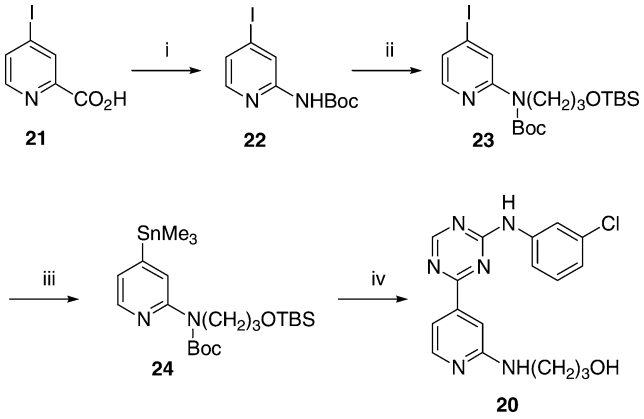

[a] (i) DPPA, Et_3N, *t*-BuOH, 65−100 °C; (ii) $Br(CH_2)_3OTBS$, Cs_2CO_3, 70 °C; (iii) Me_6Sn_2,$Pd(PPh_3)_4$, LiCl, BHT, 90 °C; (iv) (a) **4**, $Pd_2(dba)_3$, Ph_3As, BHT, toluene, 100 °C and (b) TFA.

Scheme 4[a]

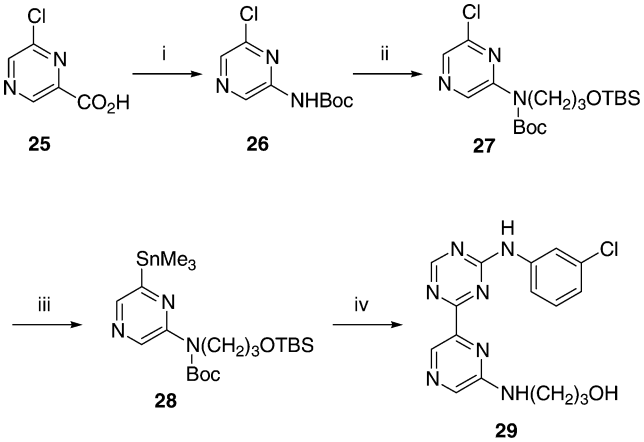

[a] (i) DPPA, Et_3N, *t*-BuOH, 65−85 °C; (ii) $Br(CH_2)_3OTBS$, Cs_2CO_3, DMF, 70 °C; (iii) Me_6Sn_2,$Pd(PPh_3)_4$, LiCl, BHT, 1,4-dioxane, 90 °C; (iv) (a) **4**, $Pd(PPh_3)_2$, LiCl, toluene, 100 °C and (b) TFA.

Cyclocondensation of **30** with (3-chlorophenyl)biguanide (**31**) gave **32**. Reaction of **32** with 3-amino-1-propanol yielded target **33**.

Scheme 5[a]

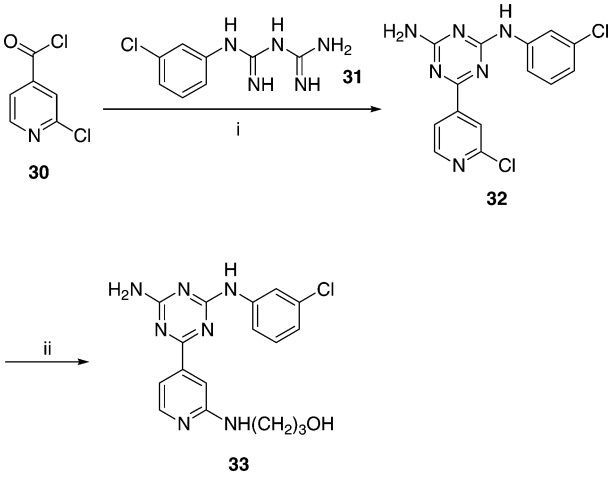

[a] (i) (3-chlorophenyl)biguanide HCl, Et_3N, THF; (ii) 3-amino-1-propanol, 100 °C.

Results and Discussion

Lead Generation. Considering the complex regulatory functions proposed for members of the CDK family and in light of the fact that no CDK inhibitor has yet received regulatory approval, it is a real challenge to predict what would be the most desirable CDK inhibitory profiles required for effective anticancer therapy. Because most CDK inhibitors that have entered clinical trials have potent CDK1 inhibitory activity, we were originally interested in identifying potent and selective CDK1 inhibitors for the treatment of cancer.[26] Following the disclosure of CGP-60474 (**37**),[27] a disubstituted pyrimidine-pyridine that has potent CDK1 inhibitory activity (IC_{50} = 0.017 μM, Chart 1) and good selectivity toward other kinases,[27] we decided to take advantage of recent advances in palladium-catalyzed C−C bond forming reactions to assemble diverse biheteroaryl molecules, which might be difficult to synthesize otherwise, with the goal to identify a new class of CDK1 inhibitors with optimized potency, selectivity, and pharmacokinetic profiles.

We unexpectedly discovered[28] the pyrazine-pyridine biheteroaryl A (compound A, Chart 1) during this exercise as a potent VEGFR-2 inhibitor but with poor CDK1 inhibitory potency (IC_{50} = 0.084 μM at VEGFR-2 and IC_{50} > 10 μM at CDK1). In contrast, the pyrimidine-pyridine biheteroaryl B (compound B) exhibited moderate CDK1 inhibitory potency but with poor VEGFR-2 inhibitory potency (IC_{50} = 2.4 μM at CDK1 and IC_{50} > 10 μM at VEGFR-2).[28] With the goal of identifying a potent CDK inhibitor, we proposed that merging the pyrimidine moiety from **37** and the pyrimidine moiety from compound B into a [1,3,5]triazine ring, may generate a potent and selective series of CDK inhibitors (target, Chart 1).

Therefore, we first synthesized triazine-pyridine **8** (Table 1), a close analogue of compound B in which the pyrimidine ring was replaced with a [1,3,5]triazine ring. Indeed, we were pleased to see the dramatic increase of CDK1 inhibitory potency of **8** (IC_{50} = 0.060 μM, Table 1) with only a moderate increase in VEGFR-2 potency (IC_{50} = 2.01 μM), as compared to compound B (IC_{50} = 2.4 μM at CDK1 and IC_{50} > 10 μM at VEGFR-2). Therefore, the addition of one nitrogen atom to the

Table 1. Inhibitory Potencies at CDK1 and VEGFR-2[a]

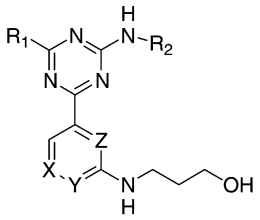

Compd	X	Y	Z	R_1	R_2	$IC_{50}(\mu M) \pm SEM(\mu M)$[b] CDK1	VEGFR-2
8	N	CH	CH	H		0.060 ± 0.020	2.01 ± 0.51
12	N	CH	CH	H	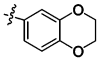	0.344 ± 0.038	4.14 ± 1.66
16	N	CH	CH	H	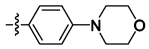	1.24 ± 0.41	5.03 ± 1.92
20	CH	N	CH	H		0.021 ± 0.006	3.50 ± 1.32
29	N	CH	N	H		0.971 ± 0.280	>10
33	CH	N	CH	NH_2		1.108 ± 0.342	1.067 ± 0.203

[a] Assay details were described in the Experimental Section. [b] SEM: standard error mean.

upper pyrimidine ring of compound B improves the CDK1 inhibition by about 40-fold.

Next, we briefly examined the impacts of various substitutions on the aniline moiety on CDK1 inhibitory potency by incorporating either a cyclic 3,4-disubstitution (compound **12**) or a 4-substitution (compound **16**). The inhibitory potencies at CDK1 for both compounds were reduced ($IC_{50} = 0.344$ μM for **12** and $IC_{50} = 1.24$ μM for **16**). It appears that the hydrophobic 3-chloro-substituent on the aniline is a more favorable choice for high CDK1 inhibitory potency.

Because the known CDK1 inhibitor **37** contains a 4-pyridine in the lower biheteroaryl, we also prepared the corresponding 4-pyridine analogue of compound **8**. Not too surprisingly, compound **20** ($IC_{50} = 0.021$ μM) is 3-fold more potent than compound **8** ($IC_{50} = 0.060$ μM) at CDK1. Meanwhile, the selectivity of compound **20** at CDK1 against VEGFR-2 is also higher than that of compound **8** (167-fold for **20** vs 34-fold for **8**). It seems that the triazine-4-pyridine **20** is a highly favorable compound that has good potency and selectivity at CDK1. In contrast, incorporation of an additional nitrogen atom in the lower pyridine ring of **8**, leading to triazine-pyrazine **29**, reduced the potency at both kinases ($IC_{50} = 0.971$ μM at CDK1 and $IC_{50} > 10$ μM at VEGFR-2). Introduction of an NH_2 group on the triazine moiety of **20**, with the intention of mimicking the N6 amino group of ATP to pick up one additional H bond with the backbone carbonyl group of Glu81,[29] also resulted in lower CDK1 inhibitory potency (**33**, $IC_{50} = 1.108$ μM).

Kinase Selectivity. We next examined the selectivity of the most potent triazine-pyridine **20** against a representative panel of kinases (Table 2). Compound **20** ($IC_{50} = 0.021$ μM) showed 3-fold higher potency at CDK2 ($IC_{50} = 0.007$ μM) and about 15-fold selectivity vs CDK4 ($IC_{50} = 0.308$ μM). Later, when tested at UBI (Upstate Biotech Inc.),[30] compound **20** exhibited comparable potency at CDK1 ($IC_{50} = 0.002$ μM)[30c] and CDK5 ($IC_{50} = 0.003$ μM), 178-fold selectivity vs CDK6 ($IC_{50} = 0.356$ μM), and 63-fold selectivity vs CDK7 ($IC_{50} = 0.126$ μM). Overall, compound **20** displayed high inhibitory potency at CDK1, CDK2, and CDK5 and with lower, but still submicromolar, potency at CDK4, CDK6, and CDK7. The broad spectrum of the CDK inhibitory activities of **20** is similar but still different to that of other CDK inhibitors, such as Roscovitine,[10] aloisines,[31] purines,[32] paullones,[33] indirubins,[34] and hymenialdisine,[35] which inhibit CDK1/CDK2/CDK5 but have much weaker or no inhibitions at CDK4/CDK6.

On the other hand, compound **20** exhibited weak or no inhibitions of 12 non-CDK kinases, with the excep-

Table 2. IC_{50} (μM) at Selected Kinase Assays[a]

kinase assay	**20**
CDK1/cyclin B	0.021 ± 0.006 (0.002)[b]
CDK2/cyclin A	0.007 ± 0.002
CDK4/cyclin D1	0.308 ± 0.054
CDK5/p35	(0.003)[b]
CDK6/cyclinD3	(0.356)[b]
CDK7/cyclinH	(0.126)[b]
calmodulin kinase II	>10
casein kinase-1	3.05 ± 1.50
casein kinase-2	>10
EGFR-1	>10
FGFR-2	>10
GSK-3β	0.020 ± 0.004 (0.003)[b]
insulin-R kinase	>10
MAPK (ERK2)	>10
PDGF-R	>10
PKA	>10
PKBβ	(>10)[b]
PKCγ	(>10)[b]
VEGFR-2	3.50 ± 1.32

[a] Assay details were described in the Experimental Section. [b] Assays were done at Upstate Biotech Inc., details were described in the Experimental Section. IC_{50} values are reported as the average of two separate determinations. See ref 30c as well.

Table 3. IC_{50} for Inhibition of Cell Proliferation[a]

cell line	$IC_{50} \pm$ SEM (μM) **20**
HeLa	0.033 ± 0.003
HCT-116	0.023 ± 0.004
U937	0.031 ± 0.006
A375	0.028 ± 0.004
MES-SA (low P-glycoprotein)	0.228 ± 0.016
MES-SA/Dx5 (high P-glycoprotein)	0.235 ± 0.003

[a] Assay details were described in the Experimental Section.

tion of potent inhibition at glycogen synthase kinase (GSK)-3β (IC_{50} = 0.02 μM, Table 2). Recently, several reports have described potent CDK inhibitors that also inhibit GSK-3β.[31,36] This was not surprising considering the high degree of homology (~86%) between the ATP-binding site of the two kinases. Since it is believed that inhibition of GSK-3β may attenuate apoptotic signals,[37] Alzheimer's disease,[38] and type-II diabetes,[39] the high inhibitory potency of **20** at GSK-3β may not be undesirable.

Cellular Activity. The cellular activity of the compound was tested by evaluating its antiproliferative effect in several established tumor cell lines. Cells tested originated from various tumor types such as HeLa (cervical adenocarcinoma), HCT-116 (colon carcinoma), U937 (monocytic leukemia), and A375 (malignant melanoma). Compound **20** demonstrated potent antiproliferative activity on all of the cell types examined (IC_{50} values ranging from 0.023 to 0.033 μM, Table 3).[40a] We also developed an assay to determine if compounds are a substrate of P-glycoprotein, the multidrug resistance pump. Induction of P-glycoprotein is the major mechanism leading to cross-resistance developing from chemotherapy. The MES-SA cell line (a drug-sensitive cell line) expresses low levels of P-glycoprotein; the MES-SA/Dx5 cell line (a drug-resistant cell line) was selected from the MES-SA cell line in the presence of doxorubicin and expresses high levels of P-glycoprotein.[40b] The ratio of IC_{50} values of the resistant cell line to the sensitive cell line indicates if the compound is a substrate for P-glycoprotein. Since compound **20** exhibited the same IC_{50} value in both cell lines (0.228 vs 0.235 μM, Table 3), it seems that **20** is not transported by P-glycoprotein.

The cellular effects of different concentrations of **20** on HeLa cells are shown in Figure 1A. HeLa cells were allowed to adhere overnight and were then treated with increasing concentrations of **20** for up to 72 h. Control cells were treated with 0.04% dimethylsulfoxide (DMSO). At 24, 48, and 72 h, cell were trypsinized and live cell numbers were determined by direct counts of trypan blue stained cells. While the number of HeLa cells in the control group (no compound **20** treatment) nearly doubled every 24 h, the growth of HeLa cells was inhibited in a dose-dependent manner when treated with **20** at concentrations ranging from 80 to 200 nM. At concentrations higher than 200 nM, compound **20** appears to exhibit toxicity to the cells because the numbers of live cells at after 24 h were lower than those at 0 h (Figure 1A).

To confirm the toxicity exerted by higher concentrations of **20**, HeLa cells were treated with 250 nM of **20** for 24 h and then divided into two groups (Figure 1B).

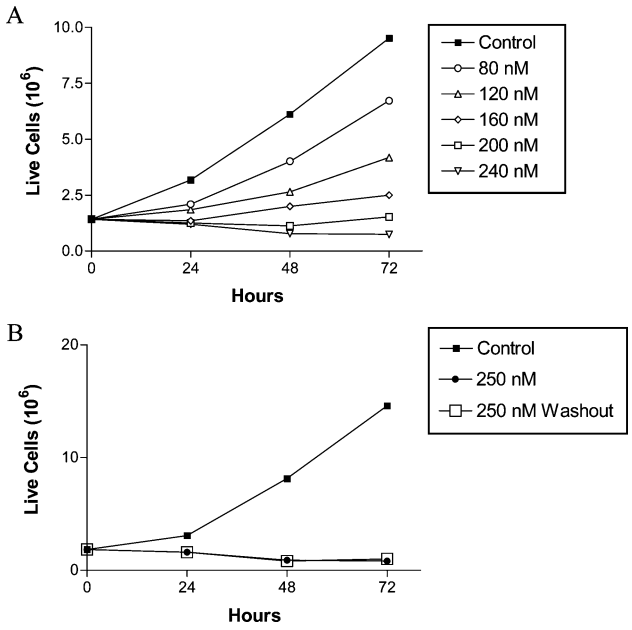

Figure 1. (A) Inhibition of cell growth by compound **20**. HeLa cells were allowed to adhere overnight and then treated with increasing concentrations of compound **20** for up to 72 h. Control cells (■) were treated with 0.04% DMSO. At 24, 48, and 72 h, cells were trypsinized and live cell numbers were determined by direct counts of trypan blue stained cells. (B) HeLa cells were treated with 250 nM of compound **20**. After 24 h, one group of cells was maintained in the presence of the drug (●) while another group was washed out of the drug and placed in fresh media containing 0.04% DMSO (□). Control cells were maintained in DMSO for the duration of the experiment (■).

One group of HeLa cells was maintained in the presence of **20** while the other group was washed free of **20** and placed in fresh media containing 0.04% DMSO. Since there was no difference in cell growth between the two groups up to 72 h, it seems that once the cells had been exposed to 250 nM concentration of **20** for 24 h, the toxic effect was irreversible even after the compound was removed.

Compound **20** was further evaluated for its ability to induce the activation of caspases in U937 human monocytic leukemia cells. Treatment of U937 cells with **20** at concentrations ranging from 0.156 to 10 μM resulted in a rapid increase in caspase activity at all of the concentrations tested in a dose-dependent manner (Figure 2). Because caspase activation is an indication of the induction of apoptosis, these data demonstrated that **20** induced apoptosis in U937 cells dose dependently from 0.156 to 10 μM.

In Vivo Antitumor Activity. The antitumor activity of **20** was evaluated in A375 human melanoma xenografts in nude mice. Although not directly related to the CDK/cyclin activity, an A375 melanoma xenograft was selected as it grows rapidly in human tumor xenografts and is representative of a type of cancer that is often difficult to treat clinically. Compound **20** was administered intraperitoneally (ip) at 150, 125, 100, 75, and 50 mg/kg once daily (qd) to end.[40c] The tumor growth delay (TGD) method was used in this study. Each animal was euthanized when its A375 neoplasm reached a size of 2.0 g. Mean day of survival (MDS) values were calculated for all of the groups. A MDS value of 33.6 days was calculated from a **20**-treated group of six mice dosed

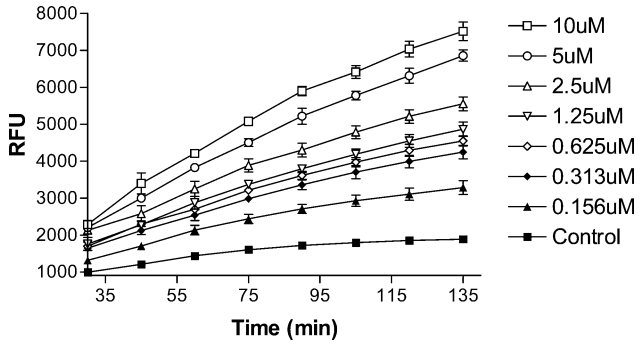

Figure 2. Caspase activation in U937 cells in the presence of compound **20**. U937 cells were plated into 96-well microplates in RPMI 1640 supplemented with 2 mM L-glutamine. Cells were exposed to various concentrations of compound **20** and incubated for 4 h at 37 °C with 5% CO_2. Control cells were exposed to vehicle only. Cells were then lysed in buffer containing caspase substrate. Free Rhodamine 110 was determined fluorimetrically at $\lambda_{max} = 521$ nm at time intervals up to 135 min. RFUs are proportional to the concentration of activated caspases 2, 3, 6, 7, 8, 9, and 10.

at 150 mg/kg and is significantly different from the vehicle control group (MDS = 21.7 days, $p = 0.004$) and represents a 55% ($p = 0.004$) survival increase. Meanwhile, the MDS value of 35.2 days of the **20**-treated group of six mice dosed at 125 mg/kg is also significantly different from the vehicle control group and represents a 62% survival increase. On the other hand, only a modest 8 day survival extension was observed with the 100 mg/kg group (MDS = 29.6 days); about the same MDS values were observed with both 75 and 50 mg/kg groups as compared to the vehicle control group. Maximal mean group body weight losses of 12−14% were recorded in all of the control groups while 5−19% weight losses were observed for the **20**-treated groups. All of the **20**-treated animal groups in these studies were tolerated within acceptable limits for the toxicity of cancer drugs in mice as set by the National Cancer Institute (NCI). In summary, the 150 and 125 mg/kg treatments of **20** each produced a statistically significant survival increase in A375-bearing mice, with one out of six mice surviving for as long as 57 days at each dose. These responses were achieved with excellent toleration. Lower doses of **20** were not efficacious, establishing a good dose response for this CDK inhibitor.

Molecular Modeling Studies. In attempts to enhance the understanding of the observed structure−activity relationships (SARs), we undertook a series of molecular docking studies on all of the compounds shown in Table 1. A model of CDK1/purvalanol B complex was built based on the X-ray structure of CDK2/purvalanol B complex (PDB code, 1CKP),[41] using the homology modeling program Prime.[42] The favorite docking pose for the representative compound **20** is illustrated in Figure 3A, while the other compounds followed the very similar docking pose. Overall, compound **20** fits nicely into the ATP-binding site of CDK1 and makes extensively favorable van der Waals contacts with the binding site through its triaryl scaffold. As shown in Figure 3A, compound **20** can adopt a typical bidentate hydrogen-bonding mode with the CDK1 backbone at the hinge region: the triazine nitrogen with the amide nitrogen of Leu83 and the anilino nitrogen with the carbonyl oxygen of Leu83. This hydrogen-bonding

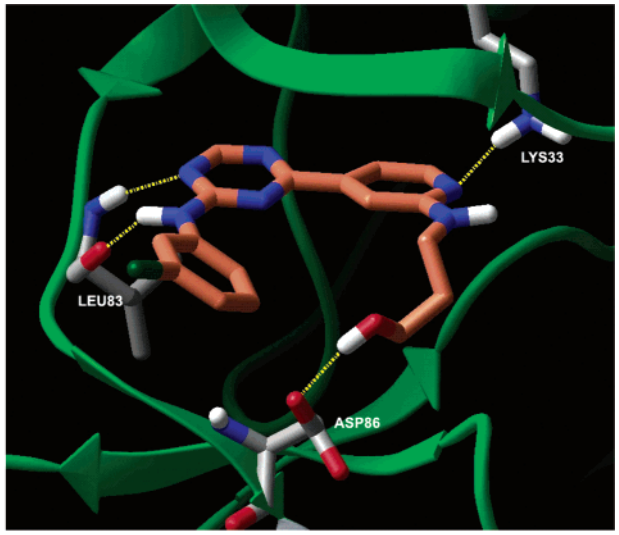

A

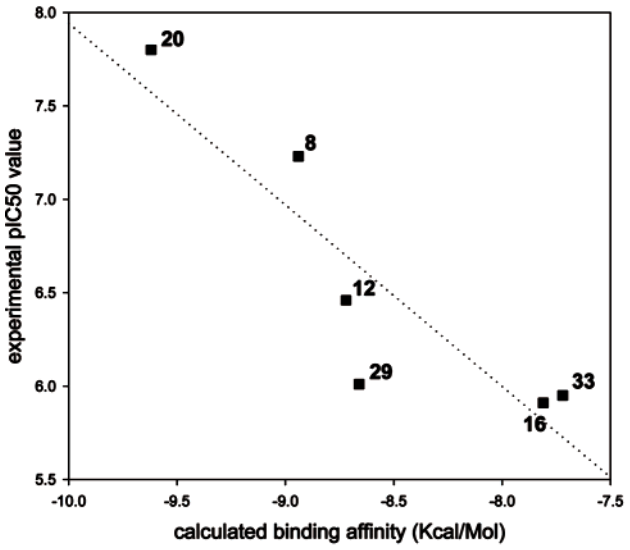

B

Figure 3. (A) Illustration of the binding mode of compound **20** in the ATP-binding site of CDK1, proposed by molecular docking. Compound **20** and its H-bonding partners (Lys33, Leu83, and Aap86) are represented in the tube model, while CDK1 is represented in the carton model. The key H bonds formed between compound **20** and CDK1 are indicated by the yellow dotted lines (atom color scheme: hydrogen in white, oxygen in red, nitrogen in blue, carbon on compound **20** in orange, and carbon on CDK1 in gray). (B) Correlation plot of the calculated binding affinities vs the experimental pIC_{50} values. The dotted line represents the best fitting line between them.

pattern is consistent with the model reported by Furet et al.[43] Two additional H bonds can also be formed between compound **20** and CDK1: one between the pyridine nitrogen and the terminal amino group of Lys33 and the other between the hydroxyl oxygen and the terminal carboxylate group of Asp86. The latter H bond reduces the tendency of a partially protonated Asp86 to form a weak H bond with the chlorine on compound **20** (the similar H bond was observed in some CDK2 X-ray structures)[41] and makes the 3-chloroanilino group favor an orientation to pack tightly against Ile10 and Phe82.

After further optimization of the CDK1 complex structures proposed by molecular docking, computational estimates of binding affinities give a fairly good correlation with the experimental data ($r^2 = 0.78$), as shown in Figure 3B. A further component analysis of these binding affinities provides some qualitative insights into the SAR observed in Table 1. Compared to compound **20**, compound **8** moves the pyridine nitrogen from the Y position to the distant X position (Table 1), which reduces the strength of the H bonding with Lys33 and leads to a decreased binding affinity ($IC_{50} = 0.060$ μM for **8** vs $IC_{50} = 0.021$ μM for **20**). Compared to compound **8**, compound **29** adds one more nitrogen at the Z position, which reduces the partial charge distribution on the X position and therefore may further decrease the H-bond strength ($IC_{50} = 0.060$ μM for **8** vs $IC_{50} = 0.971$ μM for **29**). Compound **33** has an amino group at the R_1 position, with the design intention of mimicking the N6 amino group of ATP and picking up one additional H bond with the backbone carbonyl group of Glu81. However, it turns out that this amino group is too close to the protein, and it is energetically unfavorable to form the three H bonds simultaneously with the backbone of CDK1. This may explain the unexpected observation of a higher IC_{50} value for compound **33** ($IC_{50} = 1.108$ μM). The relatively lower potencies observed for compounds **12** and **16** may attribute to the unfavorable van der Waals contacts that are induced by bulky substitutes at the para position.

Conclusion

In previous work performed in our laboratories, we identified pyrazine-pyridine A as a potent VEGF inhibitor and pyrimidine-pyridine B as a modest CDK inhibitor. A proposed combination of the pyrimidine moiety from **37** and the pyrimidine moiety from compound B led to the discovery of [1,3,5]triazine-pyridines as a new series of potent CDK inhibitors. Palladium-catalyzed C−C bond formation reactions, particularly the Negishi coupling reaction, were used to assemble various triazine-heteroaryl analogues effectively. Among them, compound **20** displayed high inhibitory potency at CDK1 ($IC_{50} = 0.021$ μM). When tested against a panel of kinases, compound **20** exhibited a broad spectrum of CDKs with inhibitory potency, that is, high potency at CDK1, CDK2, and CDK5 and with submicromolar potency at CDK4, CDK6, and CDK7. Compound **20** also displayed high potency at GSK-3β ($IC_{50} = 0.020$ μM) but weak or no inhibitions of 12 non-CDK kinases. It demonstrated potent antiproliferative activity in various tumor cell lines, including HeLa, HCT-116, U937, and A375. Because compound **20** exhibited the same IC_{50} value on both MES-SA/Dx5 and MES-SA cell lines, it appears that **20** is not a substrate of P-glycoprotein. The growth of HeLa cells was inhibited in a dose-dependent manner when treated with **20**; however, at 250 nM concentration of **20**, the toxicity effects on the cells were observed. In U937 cells, **20** induced apoptosis dose dependently via the activation of caspases. At 150 and 125 mg/kg ip doses, **20** produced a significant survival increase in A375-bearing mice, along with one mouse out of six surviving for 57 days for each dose. Molecular docking studies were conducted in an attempt to enhance the understanding of the observed SAR. The broad spectrum of potent CDK inhibitory activities, good kinase selectivity profile, high cellular potency, and the in vivo antitumor efficacy of **20** may render it as valuable pharmacological tool in elucidating the complex roles of CDK signaling pathways and the potential utility for anticancer therapy.

Experimental Section

Chemistry. ^{1}H NMR spectra were measured on a Bruker AC-300 (300 MHz) spectrometer using tetramethylsilane as an internal standard. Elemental analyses were obtained by Quantitative Technologies Inc. (Whitehouse, NJ), and the results were within 0.4% of the calculated values unless otherwise mentioned. Melting points were determined in open capillary tubes with a Thomas-Hoover apparatus and were uncorrected. Electrospray mass spectra (MS-ES) were recorded on a Hewlett-Packard 59987A spectrometer. High-resolution mass spectra (HRMS) were obtained on a Micromass Autospec. E. spectrometer. The term DMAP refers to (dimethylamino)-pyridine, NMP refers to 1-methyl-2-pyrrolidinone, DPPF refers to 1, 1′-bis(diphenylphosphino)ferrocene, $Pd_2(dba)_3$ refers to tris(dibenzylideneacetone)dipalladium(0)-chloroform adduct, and DPPA refers to diphenylphosphoryl azide.

General Prcedure for the Synthesis of 2, 10, and 14. (3-Chloro-phenyl)-carbamic Acid *tert*-Butyl Ester (2). 3-Chloroaniline **1** (29.4 g, 229 mmol) was dissolved in THF (250 mL) at 20 °C. A THF solution (80 mL) of Boc_2O (50 g, 229 mmol) was added slowly to the mixture of 3-chloroaniline and THF. The resulting mixture was stirred for 3 days and then concentrated. The crude product was purified by recrystallization from EtOAc/hexane 3 times to give 40.4 g (78%) of **2** as a white solid. ^{1}H NMR (300 MHz, $CDCl_3$): δ 7.52 (s, 1 H), 7.17 (m, 2 H), 7.00 (dt, $J = 7.4$, 1.8 Hz, 1 H), 6.49 (s, 1 H), 1.52 (s, 9 H). MS (ES) *m/z*: 250 (M + Na). Anal. ($C_{11}H_{14}NO_2Cl$) C, H, N.

General Prcedure for the Synthesis of 4, 11, and 15. (3-Chloro-phenyl)-(4-chloro-[1,3,5]triazin-2-yl)-carbamic Acid *tert*-Butyl Ester (4). THF (150 mL) was added to a mixture of compound **2** (5.5 g, 24.2 mmol) and NaH (60% in mineral oil, 2.4 g, 60.6 mmol) at 0 °C under N_2. The mixture was stirred at 20 °C for 1 h and then cooled to 0 °C and compound **3** (6.2 g, 41.2 mmol) was added. After the mixture was stirred at 20 °C overnight, the solvent was evaporated and the residue was purified by flash chromatography (10% EtOAc in hexanes) to give 4.3 g (52%) of **4** as a white solid. ^{1}H NMR (300 MHz, $CDCl_3$): δ 8.72 (s, 1 H), 7.40 (m, 2 H), 7.22 (brs, 1 H), 7.11 (m, 1 H), 1.48 (s, 9 H). MS (ES) *m/z*: 363 (M + Na). Anal. ($C_{14}H_{14}N_4O_2Cl_2$) C, H, N.

(5-Bromo-pyridin-3-yl)-carbamic Acid *tert*-Butyl Ester (6). A mixture of 5-bromonicotinic acid **5** (10 g, 49.5 mmol), *t*-BuOH (100 mL), triethylamine (15.2 g, 150 mmol), and DPPA (20.4 g, 74 mmol) in toluene (100 mL) was stirred at 65 °C for 40 min and then warmed to 100 °C for 22 h under nitrogen. The mixture was cooled and concentrated under vacuum. The crude product was purified by column chromatography on SiO_2 eluting with ethyl acetate/hexane to give 10.52 g (78%) of **6** as a white solid. ^{1}H NMR (300 MHz, $CDCl_3$): δ 8.32 (m, 3 H), 6.97 (brs, 1 H), 1.53 (s, 9 H). MS (ES) *m/z*: 273, 275 ($M + H^+$). Anal. ($C_{10}H_{13}N_2O_2Br$) C, H, N.

(5-Bromo-pyridin-3-yl)-[3-(*tert*-butyl-dimethyl-silanyloxy)-propyl]-carbamic Acid *tert*-Butyl Ester (7). A mixture of compound **6** (2.85 g, 10.44 mmol), (3-bromopropoxy)-*tert*-butyldimethylsilane (3.96 g, 15.66 mmol), and Cs_2CO_3 (10.21 g, 31.3 mmol) in anhydrous DMF (55 mL) was stirred at 70 °C for 23 h under nitrogen. The mixture was cooled, diluted with water, and extracted with ether (3 times). The organic phase was dried (Na_2SO_4) and concentrated. The product was purified by column chromatography (eluting with EtOAc/hexane) to give 4.2 g (90%) of **7** as an yellow oil. ^{1}H NMR (300 MHz, $CDCl_3$): δ 8.45 (brs, 2 H), 7.77 (brs, 1 H), 3.73 (brt, $J = 7.3$ Hz, 2 H), 3.62 (t, $J = 5.9$ Hz, 2 H), 1.81 (m, 2 H), 1.45 (s, 9 H), 0.84 (s, 9 H), 0.00 (s, 6 H). MS (ES) *m/z*: 445, 447 ($M + H^+$). Anal. ($C_{19}H_{33}N_2O_3BrSi$) C, H, N.

General Procedure for the Synthesis of 8, 12, and 16. 3-{5-[4-(3-Chloro-phenylamino)-[1,3,5]triazin-2-yl]-pyri-

din-3-ylamino}-propan-1-ol (8). *n*-BuLi (2.3 mL, 2.5 M, 5.65 mmol) was added dropwise to a solution of **7** (1.26 g, 2.82 mmol) in anhydrous THF (10 mL) at −78 °C, and the mixture was stirred for 20 min. Anhydrous zinc chloride (8.47 mL, 1 M ether, 8.47 mmol) was added dropwise to the THF solution containing **7** at −78 °C and stirred for 10 min before it was warmed to 20 °C by removing the dry ice bath. A mixture of **4** (640 mg, 1.88 mmol) and $Pd(PPh_3)_4$ (109 mg, 0.094 mmol) in dry THF (8 mL) was added. The resulting mixture was stirred at 20 °C for 10 min, then at 70 °C for 22 h, and the solvent was removed under vacuum. The residue was partitioned between water and ether and then separated. The aqueous layer was extracted with ether (3 times). The combined organic layers were dried (Na_2SO_4) and concentrated. The product (a mixture of bis-Boc- and mono-Boc- protected coupling products) was purified by column chromatography to give 458 mg of yellow foam. The yellow foam was mixed with TFA (5 mL), and the mixture was stirred at 20 °C for 2 h and then concentrated. NH_4OH was added, followed by water addition until the pH value of the aqueous layer reached about 10−11. A yellow solid was formed, collected through filtration, and then dried under vacuum. The product was purified by column chromatography to give 208 mg (73%) of **8** as a yellow solid. ^{1}H NMR (300 MHz, DMSO-d_6): δ 10.55 (s, 1 H), 8.89 (s, 1 H), 8.18 (brs, 1 H), 8.06 (s, 1 H), 7.76 (s, 1 H), 7.71 (d, J = 8.0 Hz, 1 H), 7.41 (t, J = 8.0 Hz, 1 H), 7.15 (d, J = 7.9 Hz, 1 H), 6.19 (brs, 1 H), 4.54 (t, J = 5.0 Hz, 1 H), 3.55 (m, 2 H), 3.18 (m, 2 H), 1.80 (m, 2 H). MS (ES) m/z: 357 (M + H$^+$). Anal. ($C_{17}H_{17}N_6OCl\cdot0.35H_2O$) C, H, N.

(2,3-Dihydro-benzo[1,4]dioxin-6-yl)-carbamic Acid *tert*-Butyl Ester (10). Replacing **1** with 1,4-benzodioxane-6-amine **9** and following the same procedure as in the preparation of **2** gave **10**: 71% yield. ^{1}H NMR (300 MHz, $CDCl_3$): δ 6.95 (s, 1 H), 6.77 (s, 2 H), 6.29 (brs, 1 H), 4.22 (s, 4 H), 1.50 (s, 9 H). MS (ES) m/z: 274 (M + Na). Anal. ($C_{13}H_{17}NO_4$) C, H, N.

(4-Chloro-[1,3,5]triazin-2-yl)-(2,3-dihydro-benzo[1,4]-dioxin-6-yl)-carbamic Acid *tert*-Butyl Ester (11). Replacing **2** with **10** and following the same procedure as in the preparation of **4** gave **11**: 57% yield. ^{1}H NMR (300 MHz, $CDCl_3$): δ 8.69 (s, 1 H), 6.91 (d, J = 8.5 Hz, 1 H), 6.73−6.66 (m, 2 H), 4.29 (s, 4 H), 1.49 (s, 9 H). MS (ES) m/z: 387 (M + Na). Anal. ($C_{16}H_{17}N_4O_4Cl$) C, H, N.

3-{5-[4-(2,3-Dihydro-benzo[1,4]dioxin-6-ylamino)-[1,3,5]-triazin-2-yl]-pyridin-3-ylamino}-propan-1-ol (12). Replacing **4** with **11** and following the same procedure as in the preparation of **8** gave **12**: 43% yield. ^{1}H NMR (300 MHz, DMSO-d_6): δ 10.18 (s, 1 H), 8.77 (s, 1 H), 8.68 (brs, 1 H), 8.15 (s, 1 H), 7.75 (s, 1 H), 7.68−7.36 (m, 1 H), 7.18 (brs, 1 H), 6.86 (brd, J = 8.1 Hz, 1 H), 6.17 (brs, 1 H), 4.52 (brs, 1 H), 4.24 (s, 4 H), 3.53 (m, 2 H), 3.15 (m, 2 H), 1.75 (m, 2 H). MS (ES) m/z: 381 (M + H$^+$). Anal. Calcd for $C_{19}H_{20}N_6O_3\cdot0.2H_2O$: C, 59.43; H, 5.35; N, 21.88. Found: C, 59.47; H, 5.36; N, 21.73.

(4-Morpholin-4-yl-phenyl)-carbamic Acid *tert*-Butyl Ester (14). Replacing **1** with **13** and following the same procedure as in the preparation of **2** gave **14**: 78% yield. ^{1}H NMR (300 MHz, $CDCl_3$): δ 7.26 (d, J = 8.6 Hz, 2 H), 6.86 (d, J = 8.6 Hz, 2 H), 6.31 (brs, 1 H), 3.85 (t, J = 4.7 Hz, 4 H), 3.09 (t, J = 4.8 Hz, 4 H), 1.50 (s, 9 H). MS (ES) m/z: 279 (M + H$^+$). Anal. ($C_{15}H_{22}N_2O_3$) C, H, N.

(4-Chloro-[1,3,5]triazin-2-yl)-(4-morpholin-4-yl-phenyl)-carbamic Acid *tert*-Butyl Ester (15). Replacing **2** with **14** and following the same procedure as in the preparation of **4** gave **15**: 28% yield. ^{1}H NMR (300 MHz, $CDCl_3$): δ 8.67 (s, 1 H), 7.08 (d, J = 6.9 Hz, 2 H), 6.93 (d, J = 6.9 Hz 2 H), 3.87 (t, J = 4.8 Hz, 4 H), 3.21 (t, J = 4.9 Hz, 4 H), 1.48 (s, 9 H). MS (ES) m/z: 414 (M + Na). Anal. ($C_{18}H_{22}N_5O_3Cl$) C, H, N.

3-{5-[4-(4-Morpholin-4-yl-phenylamino)-[1,3,5]triazin-2-yl]-pyridin-3-ylamino}-propan-1-ol (16). Replacing **4** with **15** and following the same procedure as in the preparation of **8** gave **16**: 4.5% yield. ^{1}H NMR (300 MHz, DMSO-d_6): δ 10.13 (s, 1 H), 8.75 (s, 1 H), 8.68 (brs, 1 H), 8.14 (s, 1 H), 7.75 (s, 1 H), 7.64 (m, 2 H), 6.97 (brs, 2 H), 6.16 (brs, 1 H), 4.53 (t, J = 5.0 Hz, 1 H), 3.75 (t, J = 4.7 Hz, 4 H), 3.54 (q, J = 6.0 Hz, 2 H), 3.19−3.09 (m, 6 H), 1.75 (m, 2 H). MS (ES) m/z: 408 (M + H$^+$). Anal. ($C_{21}H_{25}N_7O_2\cdot0.6H_2O$) C, H, N.

Method A for the Synthesis of 20. 2-Chloro-*N*-dimethylaminomethylene-isonicotinamide (18). A mixture of 2-chloroisonicotinamide **17** (4.0 g, 25.6 mmol) and *N*,*N*-dimethylformamide dimethyl acetal (3.66 g, 30.7 mmol) was heated at 100 °C for 1 h under nitrogen and then concentrated under vacuum. The residue was purified by column chromatography (EtOAc/hexane) to give 3.3 g (61%) of **18** (a mixture of the *E* and *Z* isomers) (3.3 g, 61%) as a white solid. MS (ES) m/z: 212 (M + H$^+$).

(3-Chloro-phenyl)-[4-(2-chloro-pyridin-4-yl)-[1,3,5]triazin-2-yl]-amine (19). A mixture of (3-chloro-phenyl)-guanidine nitrate (198 mg, 0.85 mmol), potassium *t*-butoxide, and THF (3 mL) was stirred at 20 °C for 15 min. Compound **18** (72 mg, 0.34 mmol) was added in one portion, and the mixture was stirred at 20 °C for 15 min and then at 70 °C for 15 min. The mixture was concentrated under vacuum. The product was purified by column chromatography (EtOAc/hexane) to give 26 mg (24%) of **19** as a solid. ^{1}H NMR (300 MHz, DMSO-d_6): δ 10.73 (s, 1 H), 8.99 (s, 1 H), 8.67 (d, J = 5.1 Hz, 1 H), 8.20 (d, J = 5.1 Hz, 1 H), 7.98 (t, J = 2.0 Hz, 1 H), 7.69 (d, J = 8.3 Hz, 1 H), 7.42 (t, J = 8.1 Hz, 1 H), 7.18 (d, J = 7.8 Hz, 1 H). Anal. ($C_{14}H_9Cl_2N_5\cdot0.1H_2O$) C, H, N.

3-{4-[4-(3-Chloro-phenylamino)-[1,3,5]triazin-2-yl]-pyridin-2-ylamino}-propan-1-ol (20). A mixture of **19** (124 mg, 0.39 mmol) and 3-amino-1-propanol (3.5 mL) was heated at 85 °C for 18 h. After water (60 mL) was added to the mixture, it was extracted with EtOAc. The organic extract was concentrated under vacuum. The residue was purified by column chromatography to give 14 mg (10%) of **20** as a yellow solid. ^{1}H NMR (300 MHz, DMSO-d_6): δ 10.58 (s, 1 H), 8.93 (s, 1 H), 8.16 (d, J = 5.3 Hz, 1 H), 7.98 (s, 1 H), 7.76 (brs, 1 H), 7.42 (m, 2 H), 7.29 (dd, J = 5.3, 1.2 Hz, 1 H), 7.16 (dd, J = 8.0, 1.3 Hz, 1 H), 6.85 (t, J = 5.5 Hz, 1 H), 4.50 (t, J = 5.2 Hz, 1 H), 3.50 (t, J = 6.2 Hz, 2 H), 3.34 (m, 2 H), 1.72 (m, 2 H). Anal. ($C_{17}H_{17}ClN_6O\cdot1.2H_2O$) C, H, N.

Method B for the Synthesis of 20. **(4-Iodo-pyridin-2-yl)-carbamic Acid *tert*-Butyl Ester (22).** A mixture of 4-iodopicolinic acid (**21**) (1.00 g, 3.30 mmol), DPPA (1.36 g, 4.95 mmol), and triethylamine (1.4 mL, 10 mmol) in *t*-BuOH (5.5 mL) and toluene (5 mL) was heated at 65 °C for 1.5 h and then 100 °C for 4 h. After concentration, the reaction mixture was purified by flash chromatography (EtOAc/hexane as the solvent) to give 515 mg (50%) of **22** as a white solid. ^{1}H NMR (300 MHz, $CDCl_3$): δ 9.17 (brs, 1 H), 8.48 (s, 1 H), 7.98 (dd, J = 5.2, 1.5 Hz, 1 H), 7.34 (dd, J = 5.2, 1.3 Hz, 1 H), 1.56 (s, 9 H). MS (ES) m/z: 343 (M + Na$^+$).

[3-(*tert*-Butyl-dimethyl-silanyloxy)-propyl]-(4-iodo-pyridin-2-yl)-carbamic Acid *tert*-Butyl Ester (23). A mixture of compound **22** (330 mg, 1.03 mmol), (3-bromopropoxy)-*tert*-butyldimethylsilane (340 mg, 1.34 mmol), and Cs_2CO_3 (504 mg, 1.55 mmol) in dry DMF (4 mL) was stirred at 70 °C for 3 h. The solvent was evaporated under reduced pressure, and the residue was purified by column chromatography (EtOAc/hexane) to provide 450 mg (89%) of **23** as a clear oil. ^{1}H NMR (400 MHz, $CDCl_3$): δ 8.11 (s, 1 H), 8.00 (d, J = 5.2 Hz, 1 H), 7.33 (dd, J = 5.2, 1.3 Hz, 1 H), 3.99 (t, J = 7.3 Hz, 2 H), 3.65 (t, J = 6.3 Hz, 2 H), 1.84 (m, 2 H), 1.52 (s, 9 H), 0.87 (s, 9 H), 0.02 (s, 6 H). MS (ES) m/z: 515 (M + Na$^+$).

[3-(*tert*-Butyl-dimethyl-silanyloxy)-propyl]-(4-trimethl-stannanyl-pyridin-2-yl)-carbamic Acid *tert*-Butyl Ester (24). A mixture of **23** (650 mg, 1.32 mmol), bis(trimethyltin) (870 mg, 2.66 mmol), tetrakis(triphenylphosphine)palladium (150 mg, 0.130 mmol), LiCl (170 mg, 4.00 mmol), and 2,6-di-*tert*-butyl-4-methylphenol (12 mg, 0.054 mmol) in anhydrous 1,4-dioxane (12 mL) was heated at 90 °C for 1.5 h under nitrogen. The solvent was removed under reduced pressure, and the residue was chromatographed over silica gel (EtOAc/hexane as the solvent) to give 590 mg (84%) of **24** as a clear oil. ^{1}H NMR (300 MHz, $CDCl_3$): δ 8.09 (d, J = 4.7 Hz, 1 H), 7.56 (s, 1 H), 7.10 (d, J = 4.7 Hz, 1 H), 3.97 (t, J = 7.2 Hz, 2 H), 3.64 (t, J = 6.5 Hz, 2 H), 1.85 (m, 2 H), 1.49 (s, 9 H), 0.86

(s, 9 H), 0.33 (s, 9 H), 0.00 (s, 6 H). MS (ES) *m/z*: 527 ($M - H^+$). Anal. ($C_{22}H_{42}N_2O_3SiSn$) C, H, N.

3-{4-[4-(3-Chloro-phenylamino)-[1,3,5]triazin-2-yl]-pyridin-2-ylamino}-propan-1-ol (20). A mixture of **4** (590 mg, 1.73 mmol), $Pd_2(dba)_3$ (160 mg, 0.175 mmol), $AsPh_3$ (424 mg, 1.39 mmol), and 2,6-di-*tert*-butyl-4-methylphenol (24 mg, 0.11 mmol) was degassed under high vacuum and then filled with N_2. This process was repeated 3 times. Toluene (20 mL) was added, and the mixture was stirred at 20 °C for about 30 min. A solution of **24** (915 mg, 1.73 mmol) in toluene (20 mL) was added, and the mixture was heated at 100 °C for 3.5 h. After removal of solvent, the residue was purified by flash chromatography (EtOAc/hexane) to give protected **20** as oil.

CF_3COOH (10 mL) was added to a solution of the protected **20** in CH_2Cl_2 (10 mL). After the mixture was stirred at 20 °C for 2 h, it was concentrated. Saturated ammonium hydroxide was added to the residue until the pH of the mixture was greater than 7. The precipitated solid was collected through filtration and washed with ice water. The crude product was purified by recrystallization from EtOAc to give 750 mg (62%) of **20** as a yellow solid. ^{1}H NMR (300 MHz, DMSO-d_6): δ 10.59 (s, 1H), 8.92 (s, 1H), 8.15 (d, J = 6.5 Hz, 1H), 7.97 (s, 1H), 7.75 (brs, 1H), 7.43 (m, 2H), 7.30 (d, J = 6.5 Hz, 1H), 7.16 (d, J = 6.5 Hz, 1H), 6.96 (brs, 1H), 4.52 (brs, 1H), 3.50 (t, J = 6.3 Hz, 2H), 3.30 (m, 2H), 1.74 (m, 2H). MS (ES) *m/z*: 357 ($M + H^+$).

(6-Chloro-pyrazin-2-yl)-carbamic Acid *tert*-Butyl Ester (26). A mixture of **25** (220 mg, 1.39 mmol), DPPA (575 mg, 2.09 mmol), and triethylamine (0.39 mL, 2.80 mmol) in *t*-BuOH (3 mL) and toluene (2 mL) was heated at 65 °C for 1.5 h, then at 85 °C for 2 h. After concentration, the mixture was purified by flash chromatography (EtOAc/hexane) to give 180 mg (57%) of **26** as a white solid. ^{1}H NMR (300 MHz, $CDCl_3$): δ 9.19 (s, 1 H), 8.26 (s, 1 H), 7.17 (brs, 1 H), 1.54 (s, 9 H).

[3-(*tert*-Butyl-dimethyl-silanyloxy)-propyl]-(6-chloro-pyrazin-2-yl)-carbamic Acid *tert*-Butyl Ester (27). A mixture of **26** (160 mg, 0.697 mmol), (3-bromopropoxy)-*tert*-butyldimethylsilane (220 mg, 0.870 mmol), and Cs_2CO_3 (340 mg, 1.04 mmol) in dry DMF (2 mL) was stirred at 60 °C for 2.5 h. The solvent was evaporated under reduced pressure, and the residue was purified by column chromatography (EtOAc/hexane) to provide 262 mg (94%) of **27** as clear oil. ^{1}H NMR (300 MHz, $CDCl_3$): δ 9.01 (s, 1 H), 8.20 (s, 1 H), 4.00 (t, J = 7.4 Hz, 2 H), 3.68 (t, J = 6.2 Hz, 2 H), 1.87 (m, 2 H), 1.54 (s, 9 H), 0.87 (s, 9 H), 0.03 (s, 6 H).

[3-(*tert*-Butyl-dimethyl-silanyloxy)-propyl]-(6-trimethylstannanyl-pyrazin-2-yl)-carbamic Acid *tert*-Butyl Ester (28). A mixture of **27** (123 mg, 0.306 mmol), bis-(trimethyltin) (200 mg, 0.611 mmol), tetrakis(triphenylphosphine)palladium (35 mg, 0.030 mmol), LiCl (40 mg, 0.94 mmol), and 2,6-di-*tert*-butyl-4-methylphenol (3 mg, 0.014 mmol) in anhydrous 1,4-dioxane (2 mL) was refluxed for 4 h under nitrogen. The solvent was removed under reduced pressure, and the residue was purified by chromatography on silica gel (EtOAc/hexane) to give 154 mg (95%) of **28** as clear oil. ^{1}H NMR (300 MHz, $CDCl_3$): δ 8.79 (s, 1 H), 8.21 (s, 1 H), 4.01 (t, J = 7.2 Hz, 2 H), 3.67 (t, J = 6.0 Hz, 2 H), 1.90 (m, 2 H), 1.53 (s, 9 H), 0.87 (s, 9 H), 0.36 (s, 9 H), 0.02 (s, 6 H). MS (ES) *m/z*: 531 ($M + H^+$).

3-{6-[4-(3-Chloro-phenylamino)-[1,3,5]triazin-2-yl]-pyrazin-2-ylamino}-propan-1-ol (29). A mixture of **28** (73 mg, 0.14 mmol), compound **4** (52 mg, 0.15 mmol), dichlorobis-(triphenylphosphine)palladium (15 mg, 0.021 mmol), and LiCl (18 mg, 0.42 mmol) in anhydrous toluene (3 mL) was stirred at 100 °C overnight under nitrogen. The mixture was cooled, concentrated under a vacuum, and purified by flash chromatography (EtOAc/hexane) to give the coupled product as yellow oil. TFA (1 mL) was added, and the mixture was stirred at 20 °C for 4 h. After it was concentrated, saturated NH_4OH solution and water were added until the mixture turned basic. After the precipitated solid was collected through filtration, it was washed with water and Et_2O and dried under vacuum to provide 1.5 mg (47%) of **29** as a yellow solid. ^{1}H NMR (300 MHz, DMSO-d_6): δ 10.59 (s, 1 H), 8.91 (s, 1 H), 8.63 (s, 1 H), 8.20 (brs, 1 H), 8.12 (s, 1 H), 7.80 (brs, 1 H), 7.39 (t, J = 8.2 Hz, 1 H), 7.34 (brs, 1 H), 7.13 (d, J = 7.8 Hz, 1 H), 4.60 (m, 1 H), 3.50 (m, 2 H), 3.32 (m, 2 H), 1.76 (t, J = 6.4 Hz, 2 H). MS (ES) *m/z*: 358 ($M + H^+$).

***N*-(3-Chloro-phenyl)-6-(2-chloro-pyridin-4-yl)-[1,3,5]-triazine-2,4-diamine (32).** To an ice-cold THF (4 mL) solution of **30** (1.66 g, 9.45 mmol) was added (3-chlorophenyl)biguanide HCl (**31**) (2.69 g, 9.45 mmol) in one portion. Et_3N (4.3 mL, 31.0 mmol) was added dropwise, and the mixture was stirred at 20 °C for 18 h. Water (10 mL) was added, and the mixture was stirred at 20 °C for 3 h and then poured into a mixture of water (50 mL) and dichloromethane (50 mL). After the solid was filtered, the dichloromethane layer was concentrated under vacuum. The resulting residue was combined with the solids and purified by column chromatography to give **32** and an unknown compound with the same R_f value (~0.5, CH_2Cl_2/MeOH = 9:1). MS (ES) *m/z*: 334 ($M + H^+$).

3-{4-[4-Amino-6-(3-chloro-phenylamino)-[1,3,5]triazin-2-yl]-pyridin-2-ylamino}-propan-1-ol (33). The less pure **32** was heated with 3-amino-1-propanol (1.6 mL) at 100 °C for 4 days. $NaHCO_3$ (25 mg) was added, and the excess 3-amino-1-propanol was removed by distillation under reduced pressure. The residue was purified by flash chromatography (CH_2Cl_2/MeOH) to give 30 mg (0.06%) of **33** as a yellow solid. ^{1}H NMR (300 MHz, CD_3OD): δ 8.02 (d, J = 5.5 Hz, 1 H), 7.96 (t, J = 2.0 Hz, 1 H), 7.63 (d, J = 8.2 Hz, 1 H), 7.43 (s, 1 H), 7.39 (d, J = 6.1 Hz, 1 H), 7.28 (t, J = 8.1 Hz, 1 H), 7.02 (d, J = 9.1 Hz, 1 H), 3.68 (t, J = 6.1 Hz, 2 H), 3.43 (t, J = 6.8 Hz, 2 H), 1.85 (m, 2 H). MS (ES) *m/z*: 372 ($M + H^+$). FAB-HRMS ($M + H^+$) calcd for $C_{17}H_{18}ClN_7O$ 372.1339, found, 372.1343.

Biology. Kinase Selectivity Assays. A kinase reaction mixture was prepared in 50 mM Tris-HCl (pH 8), 10 mM $MgCl_2$, 0.1 mM Na_3VO_4, 1 mM DTT, 0.025 μM biotinylated peptide substrate, 0.2−0.8 μCi per well 33P-γ-ATP [2000−3000 Ci/mmol], and 10 μM ATP in the presence or absence of a test compound and incubated at 30 °C for 1 h in a streptavidin coated FlashPlate (Perkin-Elmer, Boston, MA). Biotinylated peptide substrates were described as follows:[44] VEGF−R2 (Biotin-KHKKLAEGSAYEEV-Amide), Calmodulin Kinase 2 (Biotin-KKALRRQETVDAL-Amide), Casein Kinase-1 (Biotin-KRRRALS(phospho)VASLPGL-Amide), Casein Kinase-2 (Biotin-RREEETEEE-Amide), CDK1 (Biotin-KTPKKAKKPKT-PKKAKKL-Amide), CDK4 (GST-Retinoblastoma protein construct), EGFR (Biotin-DRVYIHPF-Amide), FGFR-2 (Biotin-Poly(GT) 4:1), GSK-3 (Biotin-KRREILSRRP(phospho)SYR-Amide), Insulin-R Kinase (Biotin-TRDIYETDYYRK-Amide), MAPK (Biotin-APRTPGGRR-Amide), PDGF−R (Biotin-KH-KKLAEGSAYEEV-Amide), PKA (Biotin-GRTGRRNSI-Amide), and PKCγ (Biotin-RFARKGSLRQKNV-Amide). Reaction conditions and components varied slightly depending on the protein kinase being assayed. The reaction was terminated by washing with phosphate buffered saline (PBS) containing 100 mM EDTA, and the plates were counted in a scintillation counter. Inhibition of the enzymatic activity because of the compound was measured by observing a reduced amount of ^{33}P-γ-ATP incorporated into the immobilized peptide relative to untreated controls. Linear regression analysis of the percent of inhibition by a test compound was used to calculate IC_{50} values (GraphPad Prism 3, GraphPad Software, San Diego, CA).

Protein Kinase Selectivity Panel (Upstate Biotech Inc.). Protein kinase selectivity assays were performed as previously described.[30] Briefly, protein kinases were assayed for their ability to phosphorylate the appropriate peptide/protein substrates in the presence of 10 μM compound. Assays were done using 100 μM ATP and were linear with respect to time.

Cell Culture. All of the other cell lines were from the American Type Culture Collection (Manassas, VA). Cell culture reagents were obtained from Life Technologies, Inc. (Grand Island, NY) and cells were maintained at 37 °C plus 5% CO_2 as exponentially growing monolayers in the following media supplemented with 10% fetal calf serum (Hyclone, Logan, UT) and 2 mM l-glutamine: HeLa in minimal essential

medium with 0.1 mM nonessential amino acids and 1 mM sodium pyruvate; HC-T116, MES-SA, and MES-SA/Dx5 in McCoys 5a; A375 in Dulbecco's modified Eagle's medium with 4 mM L-glutamine and 1.5 g/L sodium bicarbonate; U937 in RPMI1640.

Inhibition of Cell Proliferation. Antiproliferative activity was assessed in monolayer cultures by ^{14}C-thymidine incorporation into cellular DNA. Briefly, 5×10^3 cells were plated into 96-well scintillating microplates (Cytostar-T, Amersham Pharmacia Biotech, Buckinghamshire, U.K.) in appropriate culture medium and allowed to adhere for 24 h under standard culture conditions. Cells remained in logarithmic growth phase during the period of the assay and did not reach confluence. Test compound in DMSO was added 24 h after plating, and cells were incubated for an additional 24 h. Following this incubation, 0.2 μCi/well ^{14}C-thymidine was added and allowed to incorporate into cellular DNA for 24 h after which time the plate was washed with PBS and counted in a scintillation counter. The total time that cells were exposed to the drug was 48 h.

Caspase Activation in U937 Cells. U937 cells (5×10^4/well) were plated into 96-well microplates (Falcon Optilux, Becton Dickinson, Franklin Lakes, NJ) in RPMI 1640 supplemented with 2 mM L-glutamine. Cells were exposed to various concentrations of **20** and incubated for 4 h at 37 °C with 5% CO_2. Control cells were exposed to vehicle only. Cells were then lysed in buffer containing caspase substrate (Asp-Glu-Val-Asp-Rhodamine 110) (Roche Diagnostics, Penzberg, Germany). Free Rhodamine 110 was determined fluorimetrically at λ_{max} = 521 nm at time intervals up to 135 min. Relative fluorescence units (RFU) are proportional to the concentration of activated caspases 2,3,6,7,8,9, and 10.

In Vivo Antitumor Model. The CDK inhibitor has been submitted to the Piedmont Research Center for evaluation against the A375 human melanoma xenograft growing in nude mice. Female *nu*/*nu* mice (Harlan), 14−15 weeks of age were fed ad libitum water and an irradiated standard rodent diet (NIH 31 modified and irradiated) consisting of 18% protein, 5% fat, and 5% fiber. Female nude mice were implanted subcutaneously with 1 mm^3 A375 melanoma fragments in the flank. Tumors were monitored twice weekly and then daily as the neoplasms reached the desired size range (about 80 mg). Animals were pair matched on day 1 when their tumors were in the 62−126 mg range, and the group mean tumor sizes were 81−84 mg. Estimated tumor weight was calculated using the formula: tumor weight (mg) = $(w^2 \times l)/2$, where w = width and l = length in mm of an A375 melanoma. The CDK inhibitor **20** was provided preformulated for ip administration in a vehicle consisting of 1% PEG-2000 in water. Control groups included a no treatment tumor growth control group (10 mice) and PEG vehicle control group (10 mice). The CDK inhibitor **20** was administered ip at 150, 125, 100, 75, and 50 mg/kg on a qd × 32 schedule. No treatment control and PEG vehicle (ip, qd to end) groups were included in the test. All of the treatments were initiated on day 1, and the experiment was terminated on day 57. The TGD method was used in this study. Each animal was euthanized when its A375 neoplasm reached a size of 2.0 g. The mean day of survival (MDS) values were calculated for all of the groups. The MDS values calculated for each group based on the calculated day of death of each mouse as given by the formula

$$\text{time to endpoint (calculated)} = \text{time to exceed endpoint (observed)} - \frac{\text{Wt}_2 - \text{endpoint weight}}{(\text{Wt}_2 - \text{Wt}_1)/(D_2 - D_1)}$$

where the time to exceed endpoint (observed) = number of days it takes for each tumor to grow past the endpoint (cutoff) size (this is the day the animal is euthanized as a cancer death), D_2 = day animal is euthanized, D_1 = last day of caliper measurement before tumor reaches the endpoint, Wt_2 = tumor weight on D_2, Wt_1 = tumor weight on D_1, and endpoint weight = predetermined "cutoff" tumor size for the model being used.

Animals were weighted twice weekly during the study. Mice were examined frequently for clinical signs of any adverse, drug-related side effects. Acceptable toxicity for cancer drugs in mice is defined by the NCI as no mean group weight loss of over 20% during the test and not more than one toxic death among 10 treated animals. The unpaired t-test and Mann−Whitney U test were used to determine the statistical significance of any difference in survival times between a treatment group and the control group. All of the statistical analyses were conducted at the p level of 0.05 (two tailed). Prism (GraphPad) version 3 was used for all of the statistical analysis and for graphic presentation.

Molecular Docking Procedures. A model of CDK1/purvalanol B complex was built based on the X-ray structure of CDK2/purvalanol B complex (PDB code, 1CKP), using the homology modeling program Prime. This strategy is supported by the following facts: the amino acid sequence of human CDK1 (SWISS−PROT code, PO6493) shares a high 63% identity and 74% similarity with human CDK2 (SWISS−PROT code, P24941); it has only two different residues, Ser84 and Met85, at the ATP-binding site, as compared to CDK2; furthermore, the side chains of these two residues are extended out of the ATP-binding site and not directly involved in ligand binding. The Prime-built CDK1/purvalanol B complex structure was further optimized by full energy minimization under the environment of aqueous solution. This final structure was used as the target structure for molecular docking.

All of the the compounds were individually docked into the ATP-binding site of the above CDK1/purvalanol B model, using the docking program Glide.[45] The input structure for each compound was adopted as the lowest energy conformation determined by conformational search. The standard precision mode of Glide was used to determine the favorable binding poses, which allowed the ligand conformation to be flexibly explored while holding the protein as a rigid structure during docking. The predicted binding mode was picked from the poses that show top Emodel[46] scores and also satisfy the observed SAR. Each predicted complex structure was then fully energy minimized in the aqueous solution, with both the protein and the ligand being allowed to move. On the basis of the fully minimized structure, the binding affinity and its contribution components for each compound were recalculated using the scoring function, GlideScore.[46]

All of the the molecular mechanism calculations were done with the program MacroModel,[47] using a OPLS2001 force field.[48] The effect of aqueous solution was treated by GB/SA model.[49] The Polak−Ribiere conjugate gradient method was used for energy minimization, and the derivative convergence criterion was set at 0.05 kJ/Å-mol. Conformational search was conducted using theMonte Carlo multiple minimum method[50] as implemented in MacroModel. 5000 Monte Carlo steps were tried for each compound.

Acknowledgment. We thank Mary Pat Beavers for calculating the physical properties of some of the compounds.

Supporting Information Available: Elemental analyses data for selected compounds. This material is available free of charge via the Internet at http://pubs.acs.org.

References

(1) (a) Pardee, A. B. *Science* **1989**, *246*, 603−608. (b) Bramson, H. N.; Corona, J.; Davis, S. T.; Dickerson, S. H.; Edelstein, M.; Frye, S. V.; Gampe, Jr., R. T.; Harris, P. A.; Hassell, A.; Holmes, W. D.; Hunter, R. N.; Lackey, K. E.; Lovejoy, B.; Luzzio, M. J.; Montana, V.; Rocque, W. J.; Rusnak, D.; Shewchuk, L.; Veal, J. M.; Walker, D. H.; Kuyper, L. F. Oxindole-based inhibitors of cyclin-dependent kinase 2 (CDK2): Design, synthesis, enzymatic activities, and X-ray crystallographic analysis. *J. Med. Chem.* **2001**, *44*, 4339−4358.

(2) Morgan, D. O. Cyclin-dependent kinases: Engines, clocks, and microprocessors. *Annu. Rev. Cell Dev. Biol.* **1997**, *13*, 261−291.

(3) Hunter, T.; Pines, J. Cyclins and cancer II: Cyclin D and CDK inhibitors come of age. *Cell* **1994**, *79*, 573−583.

(4) Sielecki, T. M.; Boylan, J. F.; Benfield, P. A.; Trainor, G. L. Cyclin-dependent kinase inhibitors: Useful targets in cell cycle regulation. *J. Med. Chem.* **2000**, *43*, 1−18.
(5) (a) Nikolic, M.; Tsai, L. H. Activity and regulation of p35/cdk5 kinase complex. *Methods Enzymol.* **2000**, *325*, 200−213. (b) Maccioni, R. B.; Otth, C.; Concha, I. I.; Munoz, J. P. The protein kinase cdk5. Structural aspects, roles in neurogenesis and involvement in Alzheimer's pathology. *Eur. J. Biochem.* **2001**, *268*, 1518−1527.
(6) Napolitano, G.; Majello, B.; Lania, L. Role of cyclinT/cdk9 complex in basal and regulated transcription (Review). *Int. J. Oncol.* **2002**, *21*, 171−177.
(7) (a) Garrett, M. D.; Fattaey, A. CDK inhibition and cancer therapy. *Curr. Opin. Genet. Dev.* **1999**, *9*, 104−111. (b) Meijer, L.; Leclerc, S.; Leost, M. Properties and potential applications of chemical inhibitors of cyclin-dependent kinases. *Pharmacol. Ther.* **1999**, *82*, 279−284.
(8) (a) Senderowicz, A. M. Modulators of cyclin-dependent kinases: a novel therapeutic approach for the treatment of neoplastic diseases. *Cell Cycle Inhib. Cancer Ther.* **2003**, 179−205. (b) Wang, S.; Meades, C.; Wood, G.; Osnowski, A.; Anderson, S.; Yuil, R.; Thomas, M.; Mezna, M.; Jackson, W.; Midgley, C.; Griffiths, G.; Fleming, I.; Green, S.; McNae, I.; Wu, S.-Y.; McInnes, C.; Zheleva, D.; Walkinshaw, M. D.; Fischer, P. M. 2-Anilino-4-(thiazol-5-yl)pyrimidine CDK inhibitors: Synthesis, SAR analysis, X-ray crystallography, and biological activity. *J. Med. Chem.* **2004**, *47*, 1662−1675. (c) Nugiel, D. A.; Vidwans, A.; Etzkorn, A.-M.; Rossi, K. A.; Benfield, P. A.; Burton, C. R.; Cox, S.; Doleniak, D.; Seitz, S. P. Synthesis and evaluation of indenopyrazoles as cyclin-dependent kinase inhibitors. 2. Probing the indeno ring substituent pattern. *J. Med. Chem.* **2002**, *45*, 5224−5232. (d) Yue, E. W.; Higley, C. A.; DiMeo, S. V.; Carini, D. J.; Nugiel, D. A.; Benware, C.; Benfield, P. A.; Burton, C. R.; Cox, S.; Grafstrom, R. H.; Sharp, D. M.; Sisk, L. M.; Boylan, J. F.; Muckelbauer, J. K.; Smallwood, A. M.; Chen, H.; Chang, C.-H.; Seitz, S. P.; Trainor, G. L. Synthesis and evaluation of indenopyrazoles as cyclin-dependent kinase inhibitors. 3. Structure activity relationships at C3. *J. Med. Chem.* **2002**, *45*, 5233−5248. (e) Zhu, G.; Conner, S. E.; Zhou, X.; Shih, C.; Li, T.; Anderson, B. D.; Brooks, H. B.; Campbell, R. M.; Considine, E.; Dempsey, J. A.; Faul, M. M.; Ogg, C.; Patel, B.; Schultz, R. M.; Spencer, C. D.; Teicher, B.; Watkins, S. A. Synthesis, structure−activity relationship, and biological studies of indolocarbazoles as potent cyclin D1-CDK4 inhibitors. *J. Med. Chem.* **2003**, *46*, 2027−2030. (f) Markwalder, J. A.; Arnone, M. R.; Benfield, P. A.; Boisclair, M.; Burton, C. R.; Chang, C.-H.; Cox, S. S.; Czerniak, P. M.; Dean, C. L.; Doleniak, D.; Grafstrom, R.; Harrison, B. A.; Kaltenbach, III, R. F.; Nugiel, D. A.; Rossi, K. A.; Sherk, S. R.; Sisk, L. M.; Stouten, P.; Trainor, G. L.; Worland, P.; Seitz, S. P. Synthesis and biological evaluation of 1-aryl-4,5-dihydro-1*H*-pyrazolo[3, 4-*d*]pyrimidin-4-one inhibitors of cyclin-dependent kinases. *J. Med. Chem.* **2004**, *47*, 5894−5911. (g) Schoepfer, J.; Fretz, H.; Chaudhuri, B.; Muller, L.; Seeber, E.; Meijer, L.; Lozach, O.; Vangrevelinghe, E.; Furet, P. Structure-based design and synthesis of 2-benzylidene-benzofuran-3-ones as flavopiridol mimics. *J. Med. Chem.* **2002**, *45*, 1741−1747.
(9) Dasmahapatra, G. P.; Didolkar, P.; Alley, M. C.; Ghosh, S.; Sausville, E. A.; Roy, K. K. In vitro combination treatment with perifosine and UCN-01 demonstrates synergism against prostate (PC-3) and lung (A549) epithelial adenocarcinoma cell lines. *Clin. Cancer Res.* **2004**, *10* (15), 5242−5252.
(10) Grosios, K. UCN-01 Kyowa Hakko Kogyo Co. *Curr. Opin. Invest. Drugs* **2001**, *2*, 287−297.
(11) McClue, S. J.; Blake, D.; Clarke, R.; Cowan, A.; Cummings, L.; Fischer, P. M.; MacKenzie, M.; Melville, J.; Stewart, K.; Wang, S.; Zhelev, N.; Zheleva, D.; Lane, D. P**.** In vitro and in vivo antitumor properties of the cyclin dependent kinase inhibitor CYC202 (*R*-roscovitine). *Int. J. Cancer* **2002**, *102*(5), 463−468.
(12) Dana, G.; Vivette, D.; Tearina, C. T.; Anna, B.; Athos, G.-B.; Gelman, I. H.; Nelson, P. J. Reversal of collapsing glomerulopathy in mice with the cyclin-dependent kinase inhibitor CYC202. *J. Am. Soc. Nephrol.* **2004**, *15*, 1212−1222.
(13) Misra, R. N.; Xiao, H. Y.; Kim, K. S.; Lu, S.; Han, W. C.; Barbosa, S. A.; Hunt, J. T.; Rawlins, D. B.; Shan, W.; Ahmed, S. Z.; Qian, L.; Chen, B. C.; Zhao, R.; Bednarz, M. S.; Kellar, K. A.; Mulheron, J. G.; Batorsky, R.; Roongta, U.; Kamath, A.; Marathe, P.; Ranadive, S. A.; Sack, J. S.; Tokarski, J. S.; Pavletich, N. P.; Lee, F. Y.; Webster, K. R.; Kimball, S. D. N-(cycloalkylamino)-acyl-2-aminothiazole inhibitors of cyclin-dependent kinase 2. N-[5-[[[5-(1,1-dimethylethyl)-2-oxazolyl]methyl]thio]-2-thiazolyl]-4- piperidinecarboxamide (BMS-387032), a highly efficacious and selective antitumor agent. *J. Med. Chem.* **2004**, *47*, 1719−1728.
(14) Dittrich, C.; Dumez, H.; Calvert, H.; Hanauske, A.; Faber, M.; Wanders, J.; Yule, M.; Ravic, M.; Fumoleau, P. Phase I and pharmacokinetic study of E7070, a chloroindolylsulfonamide anticancer agent, administered on a weekly schedule to patients with solid tumors. *Clin. Cancer Res.* **2003**, *9*, 5195−5204.
(15) No structure available. Siemeister, G.; Briem, H.; Brumby, T.; Haberey, M.; Hess-Stumpp, H.; Jautelat, R.; Kruger, M.; Lucking, U.; Reichel, A.; Schafer, M.; Bosslet, K. The dual-specific CDK2/VEGF−RTK inhibitor ZK−CDK potently inhibits proliferation of human tumor cells, induces apoptosis, and inhibits growth of human xenograft tumors. *Proc. Am. Assoc. Cancer Res.* **2004**, *45*, Abst 829.
(16) Harris, R. L. N. The synthesis of triazines from *N*-cyanocarbamimidates. *Synthesis* **1981**, 907−908.
(17) Reisch, J.; Dziemba, P.; Mura, M. L.; Rao, A. R. R. Natural product chemistry. part 159 [1]. Two methods for the synthesis of 4-azaacronycine as a potential antitumor agent. *J. Heterocycl. Chem.* **1993**, *30*, 981−983.
(18) Fujita, M.; Oka, H.; Ogura, K. Palladium(0)/LiCl promoted cross-coupling reaction of (4-pyridyl)stannanes and aromatic bromides: easy access to poly(4-pyridyl)-substituted aromatics. *Tetrahedron Lett.* **1995**, *36*, 5247−5250.
(19) Littke, A. F.; Dai, C.; Fu, G. C. Versatile catalysts for the suzuki cross-coupling of arylboronic acids with aryl and vinyl valides and triflates under mild conditions. *J. Am. Chem. Soc.* **2000**, *122*, 4020−4028.
(20) Hargreaves, S. L.; Pilkington, B. L.; Russell, S. E.; Worthington, P. A. The synthesis of substituted pyridylpyrimidine fungicides using palladium-catalysed cross-coupling reactions. *Tetrahedron Lett.* **2000**, *41*, 1653−1656.
(21) Chen, C.; Dagnino, R., Jr.; McCarthy, J. R. A convenient synthetic method for trisubstituted s-triazines. *J. Org. Chem.* **1995**, *60*, 8428−8430.
(22) Hughes, J. L.; Liu, R. C.; Enkoji, T.; Smith, C. M.; Bastian, J. W.; Luna, P. D. Cardiovascular activity of aromatic guanidine compounds. *J. Med. Chem.* **1975**, *18*, 1077−1088.
(23) Lohse, O. Improved large-scale preparation of 4-iodopicolinic acid. *Synth. Commun.* **1996**, *26*, 2017−2025.
(24) Kuo, G.-H.; Connolly, P.; Prouty, C.; DeAngelis, A.; Wang, A.; Jolliffe, L.; Middleton, S.; Emanuel, S. Preparation of pyrazines as modulators of vascular endothelial growth factor (VEGF) receptor tyrosine kinase. WO 200224681 A2 20020328. CAN 136: 279477.
(25) Sato, N.; Fujii, M. Studies on pyrazines. 29[1]. High regioselective synthesis of chloropyrazines from 3-substituted pyrazine 1-oxide. *J. Heterocycl. Chem.* **1994**, *31*, 1177−1180.
(26) Monaco, E. A., III; Vallano, M. L. Cyclin-dependent kinase inhibitors: cancer killers to neuronal guardians. *Curr. Med. Chem.* **2003**, *10*, 367−379.
(27) (a) CGP-60474 exhibits lower potency at CDK2 (IC_{50} = 50−80 nM) and moderate potency at CDK4 (IC_{50} = 700 nM). Ruetz, S.; Fabbro, D.; Zimmermann, J.; Meyer, T.; Gray, N. Chemical and biological profile of dual Cdk1 and Cdk2 inhibitors. *Curr. Med. Chem.: Anti-Cancer Agents* **2003**, *3*(1), 1−14. (b) Zimmermann, J. Pharmacologically active pyridine derivatives and processes for the preparation thereof. *PCT Int. Pat.* WO 9509853 1995.
(28) Kuo, G.-H.; Wang, A.; Emanuel, S.; DeAngelis, A.; Zhang, R.; Connolly, P. J.; Murray, W. V.; Gruninger, R. H.; Sechler, J.; Fuentes-Pesquera, A.; Johnson, D.; Middleton, S. A.; Jolliffe, L.; Chen, X. Synthesis and Discovery of Pyrazine-Pyridine Biheteroaryl as a Novel Series of Potent Vascular Endothelial Growth Factor Receptor-2 Inhibitors. *J. Med. Chem.* **2005**, *48*, 1886−1900.
(29) Schulze-Gahmen, U.; De Bondt, H. L.; Kim, S. H. High-resolution crystal structures of human cyclin-dependent kinase 2 with and without ATP: bound waters and natural ligand as guides for inhibitor design. *J. Med. Chem.* **1996**, *39*, 4540.
(30) (a) Bain, J.; McLauchlan, H.; Elliott, M.; Cohen, P. The specificities of protein kinase inhibitors: an update. *Biochem. J.* **2003**, *371*, 199−204. (b) Davies, S. P.; Reddy, H.; Caivano, M.; Cohen, P. Specificity and mechanism of action of some commonly used protein kinase inhibitors. *Biochem. J.* **2000**, *351*, 95−105. (c) The 10-fold and 7-fold lower IC_{50} value obtained by UBI vs J & J at CDK1 (0.002 vs 0.021 μM) and GSK-3β (0.003 vs 0.020 μM) may be due to differences in assay conditions used, those include, peptide substrate, ATP concentration, assay format, enzyme construct, and the amount of enzyme present in the assay.
(31) Mettey, Y.; Gompel, M.; Thomas, V.; Garnier, M.; Leost, M.; Ceballos-Picot, I.; Noble, M.; Endicott, J.; Vierfond, J.-M.; Meijer, L. Aloisines, a new family of CDK/GSK-3 inhibitors. SAR study, crystal structure in complex with CDK2, enzyme selectivity, and cellular effects. *J. Med. Chem.* **2003**, *46*, 222−236.
(32) (a) Gray, N.; Wodicka, L.; Thunnissen, A. M.; Norman, T.; Kwon, S.; Espinoza, F. H.; Morgan, D. O.; Barnes, G.; Leclerc, S.; Meijer, L.; Kim, S. H.; Lockhart, D. J.; Schultze, P. Exploiting chemical libraries, structure, and genomics in the search for new kinase inhibitors. *Science* **1998**, *281*, 533−538. (b) Meijer, L. Chemical inhibitors of cyclin-dependent kinases. *Trends Cell Biol.* **1996**, *6*, 393−397.
(33) (a) Schultz, C.; Link, A.; Leost, M.; Zaharevitz, D. W.; Gussio, R.; Sausville, E. A.; Meijer, L.; Kunick, C. The paullones, a series of cyclin-dependent kinase inhibitors: synthesis, evaluation of CDK1/cyclin B inhibition, and in vitro antitumor activity. *J. Med.*

Chem. **1999**, *42*, 2909−2919. (b) Zaharevitz, D.; Gussio, R.; Leost, M.; Senderowicz, A. M.; Lahusen, T.; Kunick, C.; Meijer, L.; Sausville, E. A. Discovery and initial characterization of the paullones, a novel class of small-molecule inhibitors of cyclin-dependent kinases. *Cancer Res*. **1999**, *59*, 2566−2569.

(34) Hoessel, R.; Leclerc, S.; Endicott, J.; Noble, M.; Lawrie, A.; Tunnah, P.; Leost, M.; Damiens, E.; Marie, D.; Marko, D.; Niederberger, E.; Tang, W.; Eisenbrand, G.; Meijer, L. Indirubin, the active constituent of a Chinese antileukaemia medicine, inhibits cyclin-dependent kinases. *Nat. Cell Biol*. **1999**, *1*, 60−67.

(35) Meijer, L.; Thunissen, A. M. W. H.; White, A.; Garnier, M.; Nikolic, M.; Tsai, L. H.; Walter, J.; Cleverley, K. E.; Salinas, P. C.; Wu, Y. Z.; Biernat, J.; Mandelkow, E. M.; Kim, S.-H.; Pettit, G. R. Inhibition of cyclin-dependent kinases, GSK-3β and casein kinase 1 by hymenialdisine, a marine sponge constituent. *Chem. Biol*. **2000**, *7*, 51−63.

(36) (a) Leost, M.; Schultz, C.; Link, A.; Yong-Zhong, W.; Biernat, J.; Mandelkow, E.-M.; Bibb, J. A.; Snyder, G. L.; Greengard, P.; Zaharevitz, D. W.; Gussio, R.; Senderowicz, A. M.; Sausville, E. A.; Kunick, C.; Meijer, L. Paullones are potent inhibitors of glycogen synthase kinase-3β and cyclin-dependent kinase 5/p25. *Eur. J. Biochem*. **2000**, *267*, 5983−5944. (b) Leclerc, S.; Garnier M.; Hoessel, R.; Marko, D.; Bibb, J. A.; Snyder, G. L.; Greengard, P.; Biernat, J.; Wu, Y. Z.; Mandelkow, E. M.; Eisenbrand, G.; Meijer, L. Indirubins inhibit glycogen synthase kinase-3beta and CDK5/p25, two protein kinases involved in abnormal tau phosphorylation in Alzheimer's disease. A property common to most cyclin-dependent kinase inhibitors? *J. Biol. Chem*. **2001**, *276*, 251−260.

(37) Cross, D.; Cubert, A. A.; Chalmers, K. A.; Facci, L.; Skaper, S. D.; Reith, A. D. Selective small molecule inhibitors of glycogen synthase kinase-3 activity protects primary neurons form death. *J. Neurochem*. **2001**, *77*, 94−102.

(38) Castro, A.; Martinez, A. Inhibition of tau phosphorylation: a new therapeutic strategy for the treatment of Alzheimer's disease and other neurodegenerative disorders. *Expert Opin. Ther. Pat.* **2000**, *10*, 1519−1527.

(39) Kaidanovich, O.; Eldar-Finkelman, H. The role of glycogen synthase kinase-3 in insulin resistance and type 2 diabetes. *Expert Opin. Ther. Targets* **2002**, *6*(5), 555−561.

(40) (a) Compound **8** displayed slightly lower potency in HeLa (IC_{50} = 0.068 μM) and HCT-116 (IC_{50} = 0.098 μM) cell lines. (b) Harker, W. G.; Sikic, B. I. Multidrug (pleiotropic) resistance in doxorubicin-selected variants of the human sarcoma cell line MES-SA. *Cancer Res*. **1985**, *45*, 4091−4096. (c) The oral bioavailability of compound **20** is less than 10%, therefore, it was administered to the mice via the ip route.

(41) Gray, N. S.; Wodicka, L.; Thunnissen, A.-M. W. H.; Norman, T. C.; Kwon, S.; Espinoza, F. H.; Morgan, D. O.; Barnes, G.; LeClerc, S.; Meijer, L.; Kim, S.-H.; Lockhart, D. J.; Schultz, P. G. Exploiting chemical libraries, structure, and genomics in the search for kinase inhibitors. *Science* **1998**, *281*, 533−538.

(42) *Prime*; Schrodinger: Portland, OR .

(43) Furet, P.; Zimmermann, J.; Capraro, H.-G.; Meyer, T.; Imbach, P. Structure-based design of potent CDK1 inhibitors derived from olomoucine. *J. Comput.-Aided Mol. Des.* **2000**, *14*, 403−409.

(44) Emanuel, S.; Gruninger, R. H.; Fuentes-Pesquera, A.; Connolly, P.; Seamon, J. A.; Hazel, S.; Tominovich, R.; Hollister, B.; Napier, C.; D′Andrea, M. R.; Reuman, M.; Bignan, G.; Tuman, R.; Johnson, Moffatt, D.; Batchelor, M.; Foley, A.; O′Connell, J.; Allen, R.; Perry, M.; Jolliffe, L.; Middleton, S. A. A VEGF−R2 kinase inhibitor potentiates the activity of the conventional chemotherapeutic agents paclitaxel and doxorubicin in tumor xenograft models. *Mol. Pharmacol*. **2004**, *66*, 1−13.

(45) *Glide*; Schrodinger: Portland, OR .

(46) Friesner, R. A.; Banks, J. L.; Murphy, R. B.; Halgren, T. A.; Klicic, J. J.; Mainz, D. T.; Repasky, M. P.; Knoll, E. H.; Shelley, M.; Perry, J. K.; Shaw, D. E.; Francis, P.; Shenkin, P. S. Glide: a new approach for rapid, accurate docking and scoring. 1. Method and assessment of docking accuracy. *J. Med. Chem*. **2004**, *47*, 1739−1749.

(47) *MacroModel*; Schrodinger: Portland, OR.

(48) Jorgensen, W. L.; Maxwell, D. S.; Tirado-Rives, J. Development and testing of the OPLS all-atom force field on conformational energetics and properties of organic liquids. *J. Am. Chem. Soc.* **1996**, *118*, 11225−11235.

(49) Still, W. C.; Tempczyk, A.; Hawley, R. C.; Hendrickson, T. Semianalytical treatment of solvation for molecular mechanics and dynamics. *J. Am. Chem. Soc*. **1990**, *112*, 6127−6129.

(50) Chang, G.; Guida, W. C.; Still, W. C. An internal-coordinate Monte Carlo method for searching conformational space. *J. Am. Chem. Soc*. **1989**, *111*, 4379−4386.

JM040214H